Simulating the Evolution of Functional Brain Networks in Alzheimer's Disease: Exploring Disease Dynamics from the Perspective of Global Activity

Wei Li[1,2], Miao Wang[3], Wenzhen Zhu[4], Yuanyuan Qin[4], Yue Huang[5], Xi Chen[1,2,*]

1. School of Automation, Huazhong University of Science and Technology, Wuhan, 430074, P. R. China.

2. Image Processing and Intelligent Control Key Laboratory of Education Ministry of China, Wuhan, 430074, P. R. China.

3. China Ship Development and Design Center, Wuhan, 430064, P. R. China.

4. Department of Radiology, Tongji Hospital, Tongji Medical College, Huazhong University of Science and Technology, Wuhan, 430074, P. R. China.

5. School of Electrical and Electronic Engineering, East China Jiaotong University, Nanchang, 330013, P. R. China.

*Corresponding author E-mail: chenxi@mail.hust.edu.cn, Tel: +8618971142226.

S1. The names of the ROIs in the AAL atlas

1 Precentral_L	31 Cingulum_Ant_L	61 Parietal_Inf_L
2 Precentral_R	32 Cingulum_Ant_R	62 Parietal_Inf_R
3 Frontal_Sup_L	33 Cingulum_Mid_L	63 SupraMarginal_L
4 Frontal_Sup_R	34 Cingulum_Mid_R	64 SupraMarginal_R
5 Frontal_Sup_Orb_L	35 Cingulum_Post_L	65 Angular_L
6 Frontal_Sup_Orb_R	36 Cingulum_Post_R	66 Angular_R
7 Frontal_Mid_L	37 Hippocampus_L	67 Precuneus_L
8 Frontal_Mid_R	38 Hippocampus_R	68 Precuneus_R
9 Frontal_Mid_Orb_L	39 ParaHippocampal_L	69 Paracentral_Lobule_L
10 Frontal_Mid_Orb_R	40 ParaHippocampal_R	70 Paracentral_Lobule_R
11 Frontal_Inf_Oper_L	41 Amygdala_L	71 Caudate_L
12 Frontal_Inf_Oper_R	42 Amygdala_R	72 Caudate_R
13 Frontal_Inf_Tri_L	43 Calcarine_L	73 Putamen_L
14 Frontal_Inf_Tri_R	44 Calcarine_R	74 Putamen_R
15 Frontal_Inf_Orb_L	45 Cuneus_L	75 Pallidum_L
16 Frontal_Inf_Orb_R	46 Cuneus_R	76 Pallidum_R
17 Rolandic_Oper_L	47 Lingual_L	77 Thalamus_L
18 Rolandic_Oper_R	48 Lingual_R	78 Thalamus_R
19 Supp_Motor_Area_L	49 Occipital_Sup_L	79 Heschl_L
20 Supp_Motor_Area_R	50 Occipital_Sup_R	80 Heschl_R
21 Olfactory_L	51 Occipital_Mid_L	81 Temporal_Sup_L
22 Olfactory_R	52 Occipital_Mid_R	82 Temporal_Sup_R
23 Frontal_Sup_Medial_L	53 Occipital_Inf_L	83 Temporal_Pole_Sup_L
24 Frontal_Sup_Medial_R	54 Occipital_Inf_R	84 Temporal_Pole_Sup_R
25 Frontal_Mid_Orb_L	55 Fusiform_L	85 Temporal_Mid_L
26 Frontal_Mid_Orb_R	56 Fusiform_R	86 Temporal_Mid_R

27 Rectus_L	57 Postcentral_L	87 Temporal_Pole_Mid_L
28 Rectus_R	58 Postcentral_R	88 Temporal_Pole_Mid_R
29 Insula_L	59 Parietal_Sup_L	89 Temporal_Inf_L
30 Insula_R	60 Parietal_Sup_R	90 Temporal_Inf_R

S2. The definitions of the topological properties mentioned in the paper

The characteristic path length (*L*) represents the mean shortest path length of all nodes:

$$\mathrm{L} = \frac{2}{N(N-1)}\sum_{i>j} dis_{i,j}$$

Where the $dis_{i,j}$ represents the shortest path length between node *i* and node *j*

The clustering coefficient of node *i* is defined as:

$$C_i = \frac{n}{k(k-1)/2}$$

Where the *k* represents the number of neighbors of node *i*, and the *n* represents the number of edges among the neighbors of node *i*. The mean clustering coefficient is defined as the average value of the clustering coefficients of all nodes:

$$\mathrm{C} = \frac{1}{N}\sum C_i$$

For convenience, we call the “mean clustering coefficient” the “clustering coefficient” in our paper.

The small worldness is usually defined as the ratio of normalized mean clustering coefficient and normalized characteristic path length:

$$\mathrm{S} = \frac{C/C_0}{L/L_0}$$

Where the C_0 and L_0 represent the mean clustering coefficient and characteristic path length of a surrogate random network.

The global efficiency of a network is calculated as:

$$\mathrm{Eg} = \frac{1}{N(N-1)}\sum_{i\neq j}\frac{1}{dis_{i,j}}$$

Where the *N* represents the scale of the network, i.e. the number of nodes in the network.

S3. The ten regions that suffered most in the simulation of evolution

AAL ID	Region
57	Postcentral gyrus, left hemisphere
2	Precentral gyrus, right hemisphere
1	Precentral gyrus, left hemisphere
7	Middle frontal gyrus, lateral part, left hemisphere
4	Superior frontal gyrus, dorsolateral part, right hemisphere
8	Middle frontal gyrus, lateral part, right hemisphere
89	Inferior temporal gyrus, left hemisphere
81	Superior temporal gyrus, left hemisphere
18	Rolandic operculum, right hemisphere
29	Insula, left hemisphere

S4. Experimental results in the independent cohort *I*

As shown in Fig S1, the topological differences between the NC and AD groups were consistent with those in the primary cohort. After evolution, the topological profile of the AD group in the independent cohort *I* was well captured by the SN group.

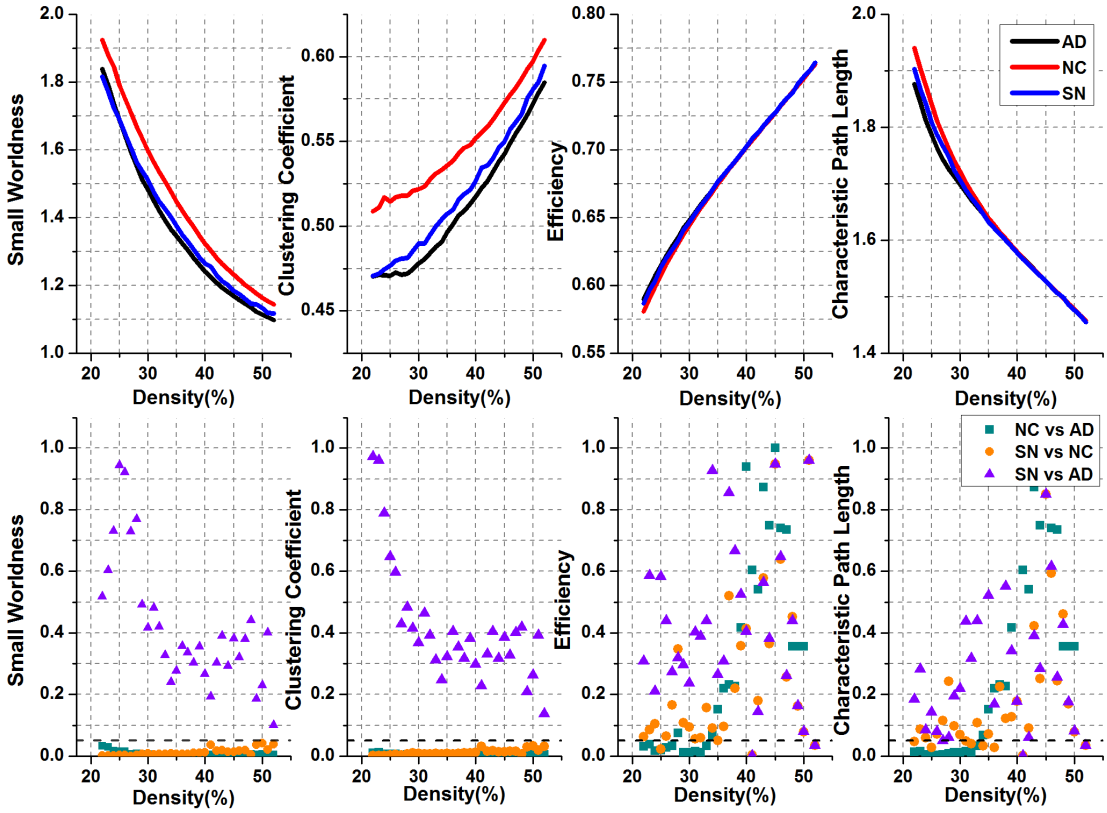

Fig S1

Meanwhile, the nodal degree distribution of the SN group approached closely that of the AD group from the initial NC group (Fig S2).

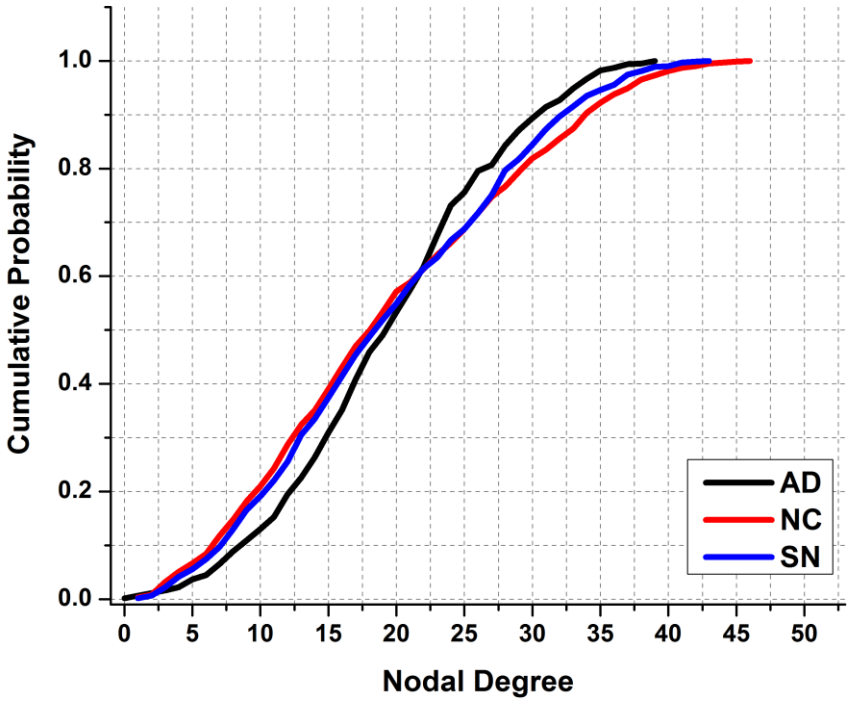

Fig S2

For comparison, after random evolution, the RN group could not fully capture the performance of the real AD group (Fig S3).

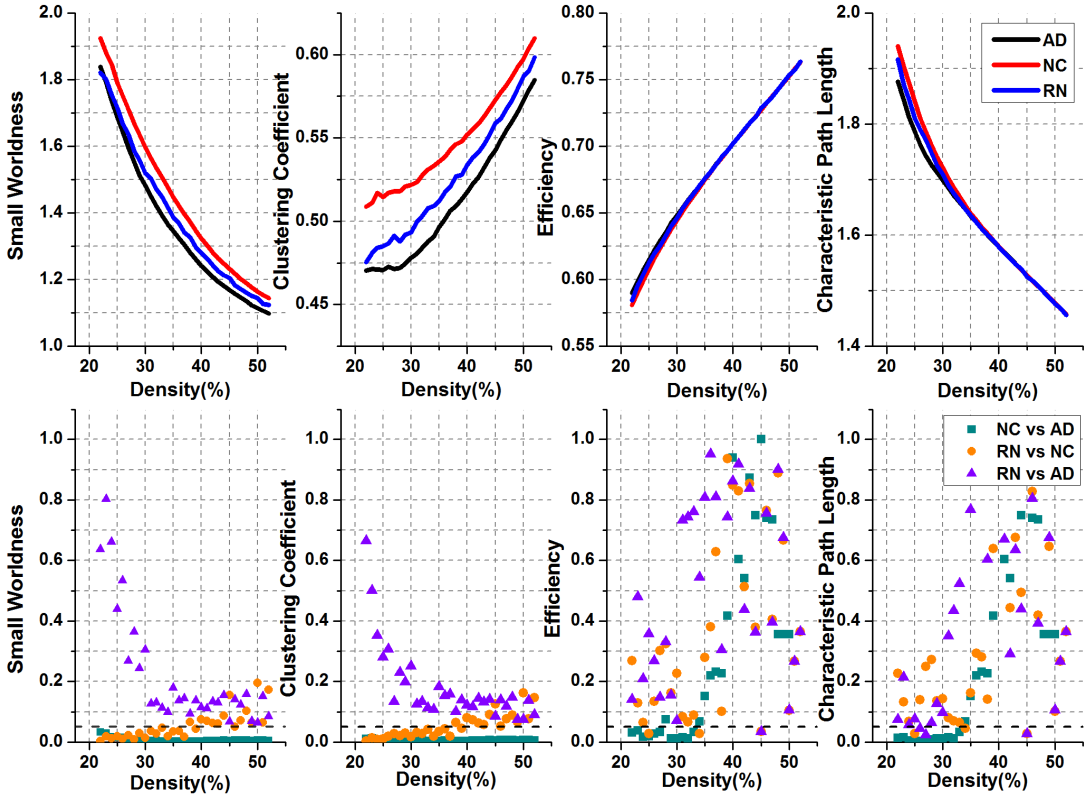

Fig S3

The results of the network attacks are consistent with those in the primary cohort, and support the conclusions in the paper (Fig S4).

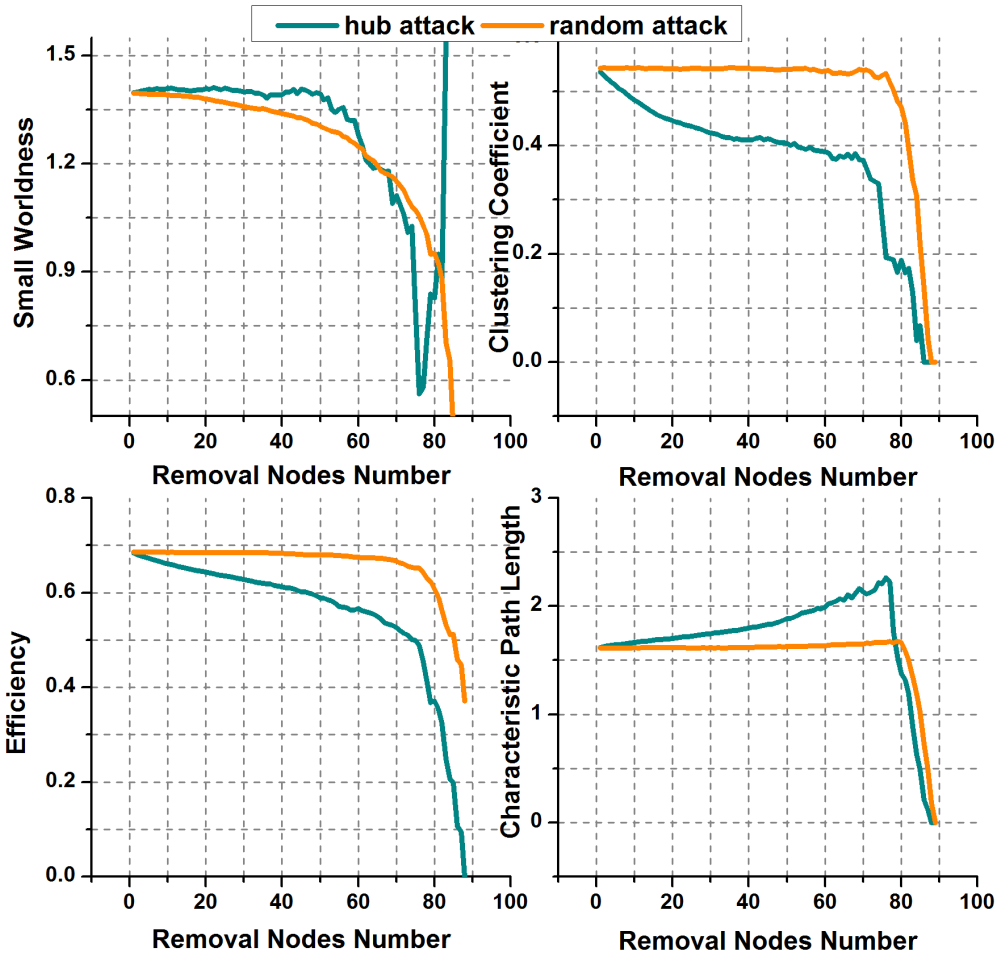

Fig S4

S5. Experimental results in the independent cohort *II*

The results (Fig S5-S8) in the independent cohort *II* were similar to those in the independent cohort *I*, and thus we do not repeat our prior explanations here.

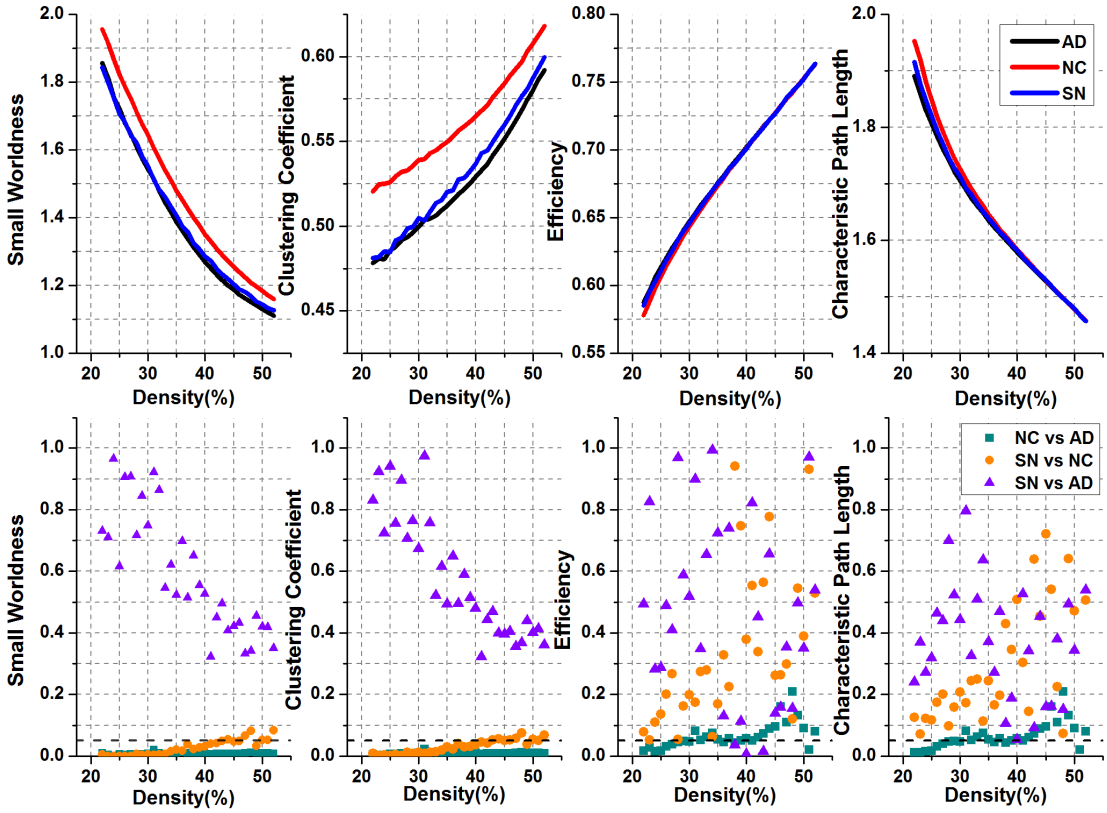
Small Worldness
Clustering Coefficient
Efficiency
Characteristic Path Length
Density(%)
AD
NC
SN
NC vs AD
SN vs NC
SN vs AD

Fig S5

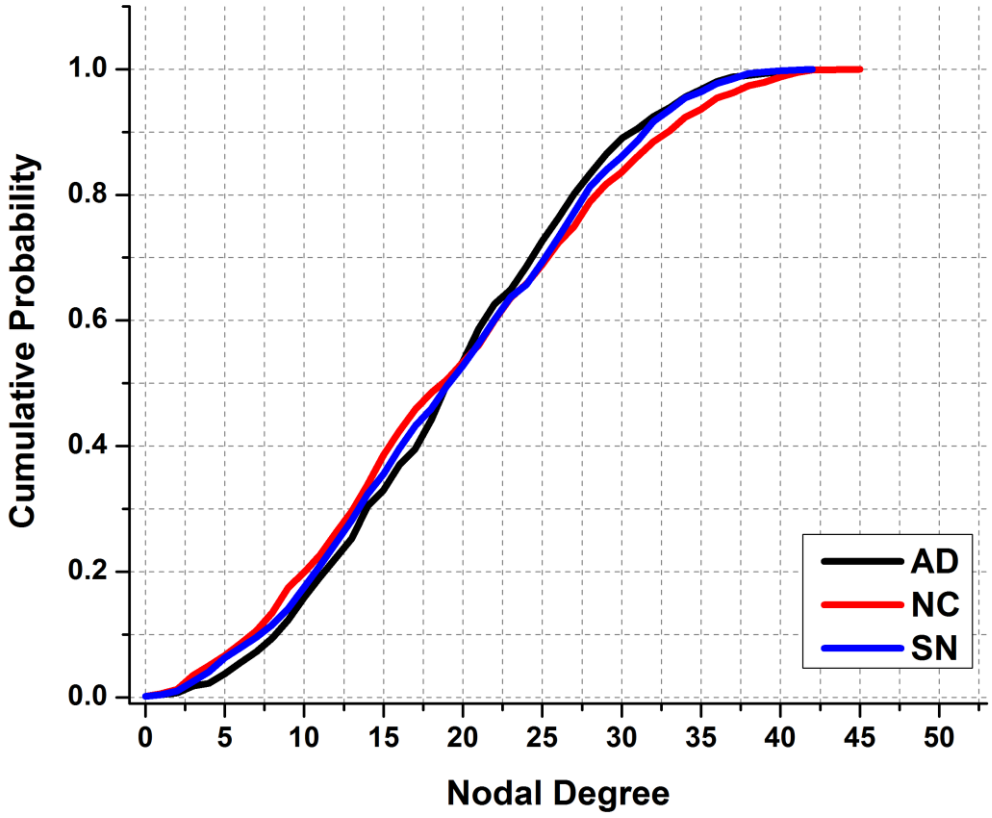
Cumulative Probability
Nodal Degree
AD
NC
SN

Fig S6

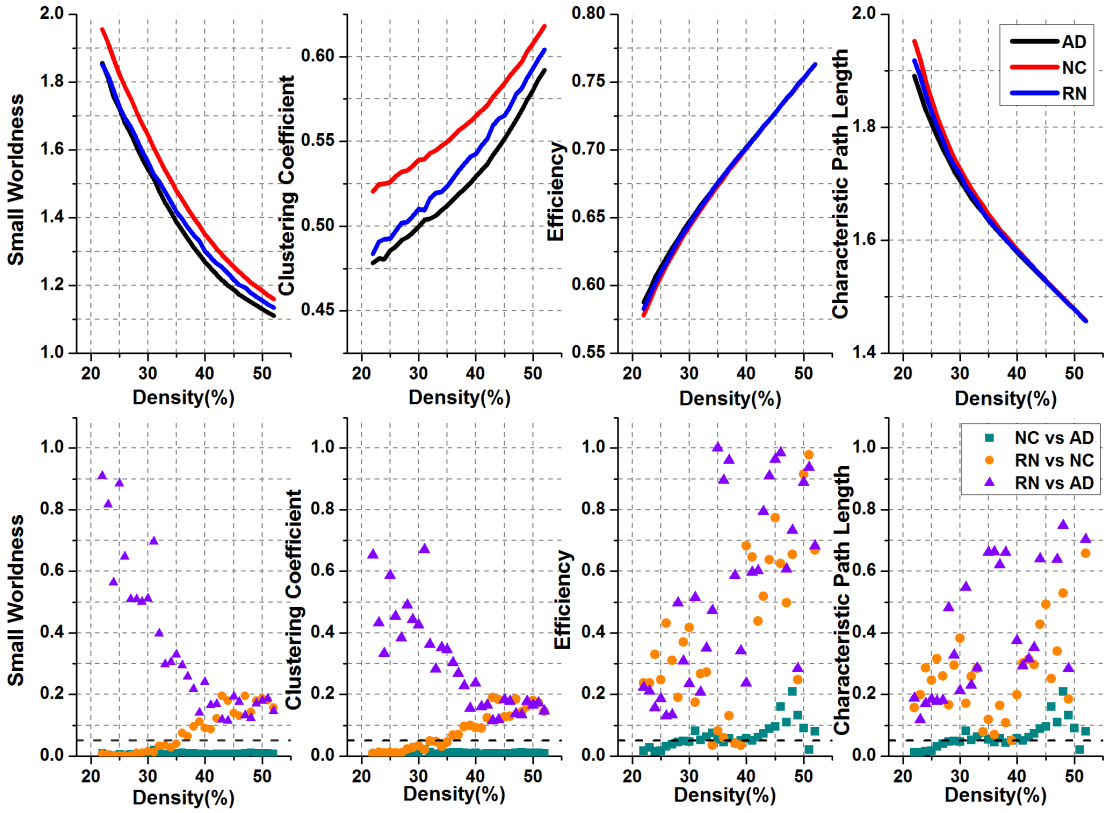
Small Worldness
Clustering Coefficient
Efficiency
Characteristic Path Length
Density(%)
AD
NC
RN
NC vs AD
RN vs NC
RN vs AD

Fig S7

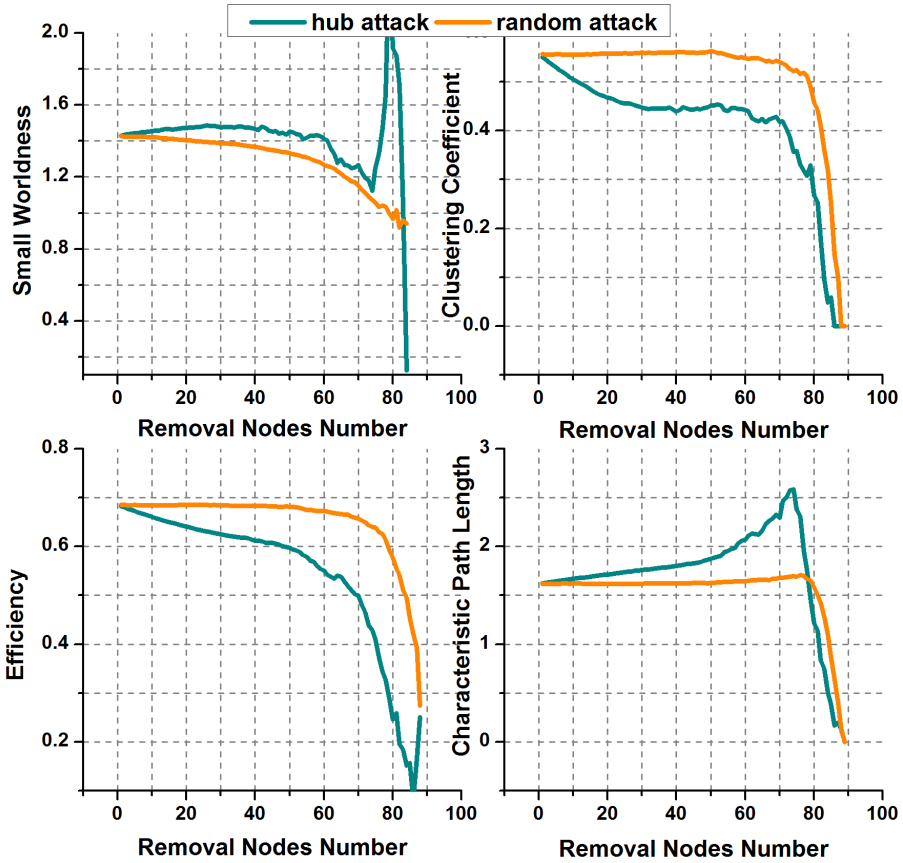
hub attack
random attack
Small Worldness
Clustering Coefficient
Efficiency
Characteristic Path Length
Removal Nodes Number

Fig S8